Environmental Science & Technology

pubs.acs.org/est

Article

Participation of Strong H-Bonding to Acidic Groups Contributes to the Intense Sorption of the Anionic Munition, Nitrotriazolone (NTO) to the Carbon, Filtrasorb 400

Wael Abdelraheem,[§] Lingjun Meng,[§] Joseph J. Pignatello,* Nourin Seenthia, and Wenqing Xu

Cite This: *Environ. Sci. Technol.* 2024, 58, 20719−20728

Read Online

ACCESS | Metrics & More | Article Recommendations | Supporting Information

ABSTRACT: 5-Nitro-1,2-dihydro-3H-1,2,4-triazin-3-one ("nitrotriazolone," NTO) is an insensitive munition compound used in modern weaponry. It poses a potential threat to soil and water quality at relevant sites due to its physical properties that cause high mobility in the environment. NTO is polar and predominantly monoanionic (NTO^-) at environmental pH (pK_{a1} = 3.64 and pK_{a2} = 11.06; determined by two independent methods in this study). Nevertheless, NTO^- sorbs strongly to the carbon, Filtrasorb 400 (Freundlich coefficient $K_F = 1.26 \times 10^4$ L^n μmol^{1-n} kg^{-1} at pH 9.5). We present evidence that sorption is contributed by the interaction of NTO^- with functional groups of similar acidity on the carbon to form exceptionally strong, negative charge-assisted hydrogen bonds, (−)CAHB, written (−$N^-\cdots H^+\cdots {}^-O$−▒), where −$N^-$ is the deprotonated N of NTO, and ^-O−▒ represents a deprotonated surface group. Behaviors consistent with (−)CAHB include (1) a "hump" in the pH-sorption profile centered around pH 4, where maximal complexation is expected to occur; (2) an apparent ∼2.4-unit upward shift in pK_{a1} due to the enhanced H-bond strength; (3) the consumption of a proton from water to form the complex; and (4) sorption suppression by competing (−)CAHB-capable solutes. Anion exchange played a minor role. The findings help advance our understanding of weak acids sorption by carbonaceous materials.

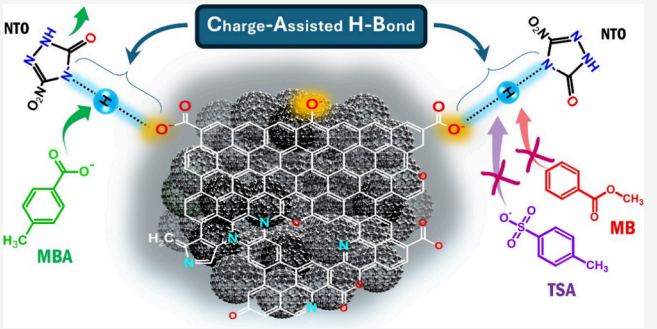

KEYWORDS: *adsorption, charge-assisted hydrogen bond, short, strong hydrogen bond, low-barrier hydrogen bond, activated carbon, insensitive munition compounds*

INTRODUCTION

Carbons are widely used for removing organic contaminants from water and mitigating their negative impacts in soil.[1,2] The meso- and microporous structure, high surface area, and hydrophobic character of the surface are key factors in the effectiveness of carbons as sorbents.[3] While solvophobic and pore-filling theories can explain the sorption of apolar and many neutral polar compounds to carbon, they do not do so well in predicting the sorption of ionic and ionizable compounds.[4−8] The sorption of ionic and ionizable compounds is far more sensitive to sorbent functional group composition, pH, ionic strength, and other ions present.[9]

Nitrotriazolone, 5-nitro-1,2-dihydro-3H-1,2,4-triazin-3-one (NTO), belongs to the category known as insensitive (fire- and shock-resistant) munitions compounds (IMC). IMC are replacing legacy munitions in modern weaponry.[10] NTO exists predominantly as the monoanion (NTO^-) at environmentally relevant pH (see sec3.1. The neutral form of NTO is highly hydrophilic; its computed octanol-water partition coefficient (log K_{ow}) lies between −1.99 and −1.19,[11] and its water solubility at 19 °C is 12.8 g/L.[12] Soluble salts of NTO^- likely have much lower log K_{ow} values and much higher water solubilities, but experimental data are unavailable. In addition, NTO interacts weakly with most geosorbents.[13−15] These properties suggest that NTO is highly mobile in the environment, though there are few, if any, reports on NTO concentrations near affected sites or attempts to predict NTO mobility.

The sorption of weak acids that dissociate to a conjugate anion by pyrogenic carbonaceous materials (PCM; incorporating engineered carbon, natural chars, and biochars) is generally pH-dependent due to ionization of the acid and variable surface charge controlled by the ionization of dissociable O,N groups, such as phenolic, carboxylic, heterocyclic amine, and others.[16,17] Most PCMs have surfaces that are net-negatively

Received: July 11, 2024
Revised: October 17, 2024
Accepted: October 18, 2024
Published: November 6, 2024

Downloaded via CENTERS DISEASE CONTROL & PRVNTN on December 10, 2024 at 15:08:28 (UTC).
See https://pubs.acs.org/sharingguidelines for options on how to legitimately share published articles.

ACS Publications

© 2024 American Chemical Society

https://doi.org/10.1021/acs.est.4c07055
Environ. Sci. Technol. 2024, 58, 20719−20728

charged at the pH values typically encountered in the environment. Sorption models regard the neutral form of the weak acid to have far higher affinity than the corresponding anionic form due to the hydrophilic nature of the anion and its repulsion by the negatively charged surface.[18,19] In a study of the carbon Filtrasorb 400 (F400), however, we observed unexpectedly strong sorption of NTO^-. In fact, the sorption of NTO^- was only slightly weaker than the sorption of uncharged NTO. This was surprising, given the polar and ionic nature of NTO^- and the negative surface charge of F400 under the slightly alkaline conditions of the experiment. This work reports efforts to explain this observation. Using various approaches, we provide evidence consistent with the contribution of exceptionally strong hydrogen (H) bonds between NTO and surface acidic groups known as negative charge-assisted H-bonds, (−)CAHB. The (−)CAHB comprises a proton and a pair of weak acid anions with comparable pK_a values, within ∼3 units according to the "ΔpK_a rule".[20−22] It can be written ($X^-\cdots H^+\cdots{}^-Y$), where X and Y are heteroatoms, usually O or N; for example, between two carboxylate ions, $RCO_2^-\cdots H^+\cdots{}^-O_2CR$. The (−)CAHB falls into the class of H-bonds known as 'short, strong' or "low-barrier" H-bonds, which owe their exceptional strength compared to ordinary H-bonds to the nearly equal sharing of the proton, which gives the bond considerable covalent character.[21,23−25] In the present case, the interacting atoms are the charged N of the NTO ring and a surface O belonging to an acidic group having a pK_a near the pK_{a1} of NTO, such as carboxyl, lactone, pyrone, or hydroxyl,

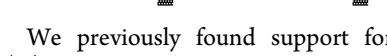

(1)

We previously found support for the involvement of a (−)CAHB in the sorption of carboxylic acids to carbonaceous materials including carbon nanotubes and biochars.[16,26−30] We report here several lines of evidence supporting the formation of a (−)CAHB with the N-centered organoanion of NTO. To our knowledge, there is no peer-reviewed literature on the sorption of NTO by carbons.

EXPERIMENTAL SECTION

Materials. 5-Nitro-1,2-dihydro-3*H*-1,2,4-triazol-3-one ("nitrotriazolone," NTO, 95%) was obtained from ENAMINE Ltd. [We note that NTO is incorrectly named in many papers as "3-nitro-1,2,4-triazol-5-one." The incorrect name is, instead, that of the dehydro compound, which would result from removing two H atoms from NTO and forming a second double bond in the ring.] The NTO standard was obtained from AccuStandard (New Haven, Connecticut, USA). 4-Methylbenzoic acid (MBA, 98%), methyl benzoate (MB, 99%), 3,5-dinitrobenzoic acid (DNBA, 98.5%), 4-acetylbenzoic acid (ABA, 98.8%), and *p*-toluene sulfonic acid (TSA, 98.5%) were obtained from Thermo Fisher Scientific. FILTRASORB 400-mesh granular-activated carbon (hereafter, F400) was obtained from Calgon Carbon. The water used was 18.2 MΩ cm ultrapure water (Millipore system). Analyte concentrations were determined by high-performance liquid chromatography (Table S1 of the Supporting Information (SI)).

Quaternary ammonium (QA)-functionalized F400 sorbents were prepared by published methods.[31] pDADMAC-F400 was made by adsorbing poly(diallyldimethylammonium) chloride from an aqueous solution. F400-Q188 (R = H) and F400-Q360 (R = cocoalkyl) were prepared by base-catalyzed coupling of epoxide precursors to surface hydroxyl groups:

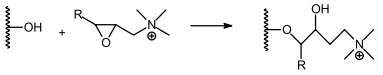

(2)

Acidity Constants by Spectrophotometric and Potentiometric Titrations. Spectrograms were recorded for a series of NTO solutions (320 μM) adjusted to different pH from 1.9 to 12.7 with freshly prepared solutions of KOH or HCl, while maintaining constant ionic strength (IS) of 100 mM adjusted with NaCl. Blanks without NTO were adjusted to the same pH and IS. Spectrograms were mathematically deconvoluted using the *"Shirley"* function of SigmaPlot (Alfasoft), to resolve the exact absorbance values of each NTO species. After deconvolution, the data were normalized and then fitted with Excel Solver to minimize differences between the calculated and experimental spectra (species α value, percent of total NTO) at the wavelengths characterizing each NTO species. Calculated absorbance data were generated by summing the product of each species' α calculated from the predicted acidity constants of NTO, using the first-guessed values.

A modified Kraft method[32] was used for potentiometric titration. The change in pH of an aqueous solution (15 mL) of NTO (500 μM) at 25 °C was recorded as a function of the added volume of freshly prepared KOH standardized against oxalic acid. The method can be used to determine pK_a values of multiprotic weak acids even when no distinct inflections and buffer regions exist in the titration curve. It involves converting the titration curve to a plot of the fraction of dissociable protons bound to the weak acid, n_H, as a function of pH. The equation for the difference plot for a diprotic acid is written as follows,

$$n_H = \frac{\text{moles of bound } H^+}{\text{total moles of weak acid}} = n + \frac{-c_b v - (10^{-pH} - 10^{(-pK_w+pH)})(v_0 + v)}{[NTO]_T} \quad (3)$$

where n is the number of H^+ bound to weak acid, c_b (M) is the added KOH concentration, v (L) is the volume of added KOH, K_w is the acidity constant of water (1×10^{-14} at 25 °C), v_0 (L) is the initial volume, and $[NTO]_T$ (M) is the total NTO concentration (taking into account dilution by an added base).

NTO Sorption Experiments. F400 (0.25 g/L) was prewetted in ultrapure water in sealed polypropylene vials at room temperature for 1 week, periodically adjusting the pH with HCl and/or NaOH to the desired value. The vials were then spiked with the NTO stock solution at the same pH. The final volume was adjusted to 40 mL with an IS of 100 mM with NaCl. Buffers were not used to avoid potential interference by the buffer ions.

Vials were mixed end-over-end at 40 rpm at 25 °C for 5 days, during which time the pH stabilized. We regarded this as sufficient time to approach equilibrium. Samples of the solution were filtered (0.45 μm PTFE) prior to NTO analysis. Sorbed NTO was calculated by subtracting the mass in solution from the mass added, assuming no losses. Data were fit to the Langmuir (eq 4) and Freundlich (eq 5) models,

$$C_s = \frac{K_L S_{LM} C_w}{1 + K_L C_w} \quad (4)$$

$$C_s = K_F C_w^{\,n} \quad (5)$$

https://doi.org/10.1021/acs.est.4c07055
Environ. Sci. Technol. 2024, 58, 20719−20728

where C_s (μmol/kg) and C_w (μmol/L) are the sorbed and dissolved concentrations, respectively; S_{LM} (μmol/kg) and K_L (L/μmol) are Langmuir maximum capacity and affinity coefficients, respectively; K_F (μmol/kg)(μmol/L)$^{-n}$ is the Freundlich sorption coefficient; and n is the Freundlich linearity index. The Langmuir model assumes monolayer adsorption on a homogeneous surface with a finite number of sites, while the Freundlich model assumes a multiplicity of sites distributed in energy.[33] Equation 4 was solved by nonlinear least-squares regression. Equation 5 was solved by linear least-squares regression of the log-transformed form of eq 5. In both cases, data were weighted by the dependent variable. The accuracy of fitting in both models was tested using the adjusted (for degrees of freedom) coefficient of determination R^2_{adj}. The observed (concentration-dependent) distribution ratio K_d (L/kg) is defined as the NTO sorbed-to-solution concentration ratio, which, if not determined experimentally, can be calculated from the Freundlich K_F by eq 6.

$$K_d = \frac{C_s}{C_w} = K_F C_w^{\,n-1} \tag{6}$$

Competitive sorption experiments were performed by mixing NTO (10 μmol/L) and a competitor (MBA, MB, TSA, ABA, or DNBA; 10−950 μM) with F400 (5.0 or 1.0 g/L) that had been prewetted and pH-adjusted to pH 7.0 and 100 mM IS (NaCl), as above. Again, buffers were not used to eliminate possible interference. After 1 week mixing at 25 °C, pH had stabilized between 6.41 and 6.82, and NTO and competitor concentrations in filtered liquid samples were quantified.

pH Drift Experiments. Stock solutions of 1 M NaCl and 0.1 M NTO were prepared, and each was adjusted to pH 5.0. Water suspensions of F400 were allowed to equilibrate for 1 week, with adjusting the pH daily with HCl and NaOH until it stabilized at a target pH of 5.0. Equilibration is slow due to carbon's strong buffering capacity and the slow diffusive equilibration of protons into its pores. The target pH was chosen to ensure NTO's predominance in anionic form and to correspond to a point of maximum likelihood of CAHB formation, which is near the mean of the pK_a of NTO and the "average" pK_a of acidic groups to which a CAHB could be formed. Following pH stabilization, NaCl and NTO stock solutions were added to the F400 suspension to initiate the experiment. Final concentrations were 22.5 mg/L F400, 50 mM NaCl, and 0 (the control), 500, 1000, or 2000 μM NTO, each in duplicate. The observed initial pH of the samples and control ranged from 4.89 to 5.10. Measurements of the pH were recorded at predetermined times over 96 h. The arithmetic average $[H^+]$ was used for subsequent calculations ($pH_{ave} = -\log[(10^{-pH_1} + 10^{-pH_2})/2]$, where 1 and 2 represent the first and second duplicates). Reproducibility was excellent, with the average difference between duplicates being only 1.7% of a pH unit (range, 0.02−3.5%). The sorbed concentration of NTO at each time point was calculated from NTO measured in an aqueous subsample and the total mass added.

To determine the buffering capacity of F400, suspensions of F400 were pre-equilibrated for 1 week with small additions of HCl until they stabilized at pH 4.5. A blank without F400 was also prepared. Subsequently, each sample and a corresponding blank received a pH 4.5-adjusted NaCl stock solution and incremental amounts of standard NaOH solution. Final concentrations were 22.5 mg/L F400 and 50 mM NaCl. Measurements of pH were taken at the same times as those in the pH drift experiment. An example is shown in Figure S1.

RESULTS AND DISCUSSION

NTO Acidity Constants. Acidity constants are key chemical properties that are essential for interpreting the results for NTO here. In 1987, Lee et al. introduced NTO as a new munition compound that behaved as a monoprotic weak acid with a pK_a of 3.67, a value unaccompanied by experimental data.[34] In 1997, Le Campion et al. obtained a pK_a of 3.7 by capillary electrophoresis.[35] In 1999, Smith et al. assumed the value of 3.76, citing an unreachable technical report.[36] In 2015, Golius et al. estimated a pK_a of 4.28 at 298.15 K computationally from the Gibbs free energy of deprotonation of tautomeric structures in water.[37] In 2021, Murillo-Gelvez et al. reported a second deprotonation constant (pK_a 11.25),[38] citing an unreachable article published in 1980[39] and a second, accessible article published in 1996[40] that did not acknowledge any second pK_a for NTO. While the present work was in progress, a paper appeared in 2023 reporting a second pK_a of 10.9 ± 0.3 determined spectrophotometrically.[41] The present study pinpoints the pK_{a1} and pK_{a2} values of NTO to a high level of accuracy using two independent methods—spectrophotometric titration and potentiometric titration—thereby clearing up the sparse and confusing literature regarding pK_{a1} and reducing the uncertainty in the recently reported[41] value of pK_{a2}.

The absorption spectra between 200 and 650 nm of 320 μM NTO at different pH 1.9−12.7 are shown in Figure S2A. Solutions gradually changed from colorless to yellow to dark reddish-brown over the pH range. We note that NTO is chemically stable for at least a week at pH 13.8, so the color change is due to speciation, not reaction. Absorbances at peak maxima of 226, 270, 315, 345, and 411 nm as a function of pH are plotted in Figure S2B. Two inflections appear, indicating that NTO has two ionizable protons (eqs 7 and 8).

$$NTO \rightleftharpoons NTO^- + H^+; \quad K_{a1} = \frac{[NTO^-][H^+]}{[NTO]} \tag{7}$$

$$NTO^- \rightleftharpoons NTO^{2-} + H^+; \quad K_{a2} = \frac{[NTO^{2-}][H^+]}{[NTO^-]} = \frac{[NTO^{2-}][H^+]^2}{[NTO]} \tag{8}$$

The observed absorbance at a given pH generally represents a mixture of NTO species. To deconvolute the spectra, we first chose 315, 345, and 411 nm to represent NTO, NTO^-, and NTO^{2-}, respectively (Figure S3A−C). After spectral deconvolution, the resulting absorbance values are plotted as a function of pH (Figure S3D). Normalization and then fitting were performed using the first-guessed values of 3.0 and 11.0 for pK_{a1} and pK_{a2}, respectively. Figure 1A shows a plot of experimental (exp) and calculated (cal) α (where $\alpha = [NTO^n]/[NTO_T]$, %, for n = 0, 1-, or 2-) of each species, with pK_{a1} and pK_{a2} estimated to be 3.68 and 11.06, respectively.

For potentiometric titration, the difference plot protocol of Kraft[32] converts the titration curve (Figure S4) to a plot of the fraction of dissociable protons bound to the weak acid, n_H, as a function of pH (Figure 1B). The values of pK_{a1} = 3.61 and pK_{a2} = 11.1 are found at n_H = 1.5 and 0.5, respectively (see eq 3). These values are in excellent agreement with the

https://doi.org/10.1021/acs.est.4c07055
Environ. Sci. Technol. 2024, 58, 20719−20728

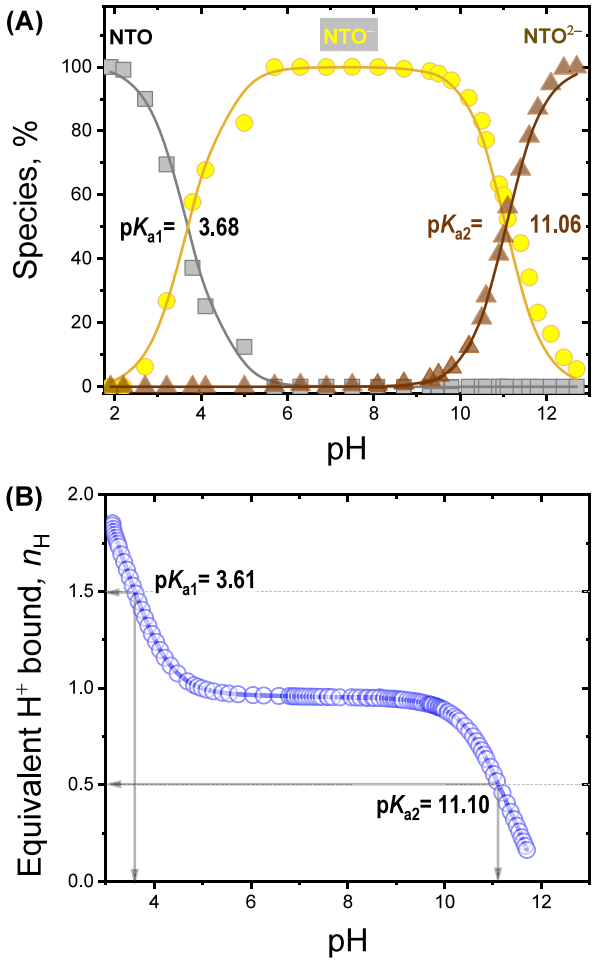

Figure 1. Acidity constants pK_{a1} and pK_{a2} of NTO determined by two independent methods (5.0 mM NTO; ionic strength 100 mM (KCl); 25 °C). (A) Spectrophotometric titration. Plot of speciation as a function of pH. The points are experimental values from Figure S2E, and the solid lines are fits. (B) Potentiometric titration. Difference plot for NTO.

corresponding values obtained by the spectrophotometric method.

Based on molecular computations,[37] the most stable structure of the monoanion is the one shown in Figure 2, where the charge is centered on N and partially delocalized into the C═O and C═N bonds. Our results yield pK_{a1} in agreement with the "pK_a" determined by capillary electrophoresis reported in 1997.[35] Our results confirm the second acid dissociation constant reported in 2023.[41] However, they provide values of pK_{a1} and pK_{a2} of greater accuracy and confidence because they were determined by two independent methods that closely agree. Taking the arithmetic means of K_{a1} and K_{a2} determined by the two different methods, we assign pK_{a1} to be 3.64 and pK_{a2} to be 11.08.

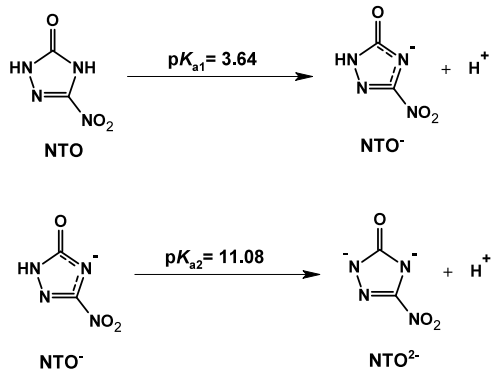

Figure 2. Deprotonation reaction and assigned pK_a values of NTO.

Sorption Isotherms. The sorption isotherm of NTO is presented at two different pH values in Figure 3—pH 1.41−1.52, where NTO is predominantly neutral, and pH 9.5, where NTO is predominantly monoanionic (i.e., no participation of NTO^0) and well above the isoelectric point of F400 (pH 4.5).[42] We focused on low concentrations of NTO (~1 μM to ~1 mM) relative to NTO's water solubility (>100 mM) to probe the carbon's affinity rather than capacity for NTO and because such concentrations are more relevant to situations in which carbons would be used to clean up contaminated soil, natural waters, or wastewater streams. Based on R_{adj}^2, the Freundlich fits are slightly better than the Langmuir fits in each case. Both models show that neutral NTO has a greater affinity for F400 than does NTO^-: Freundlich log K_F (4.64 vs 4.09) and Langmuir log ($S_{LM}{\cdot}K_L$) (3.99 vs 3.73). However, the Langmuir capacity S_{LM} is smaller for neutral NTO than for NTO^- (1.91 vs 3.92 mol/kg). Based on the Freundlich model, the distribution ratio K_d for NTO^- at pH 9.5 is $\geq 10^4$ L/kg below ~0.4 mg/L (3.08 μM) NTO^- and $\geq 5 \times 10^3$ L/kg below ~10.6 mg/L (81.5 μM) NTO^-. These values are remarkably high for a species that is negatively charged and otherwise highly polar ((O + N)/C = 0.78). It is unexpected also in view of the surface charge of F400. The isoelectric point is pH 4.5.[42] A zeta potential-pH curve (pH 2−11) shows a nearly linear decline in the zeta potential above pH 4.5 that levels off at about −32 mV at pH 9.0.[43] Finally, F400 has no significant anion exchange affinity for perchlorate (ClO_4^-) above pH 9.0,[43] Taken together, these facts mean that NTO adsorption is likely attributable to mechanisms other than anion exchange.

Conventional reasons for the widely held belief that organoanions are much more weakly sorbed than the undissociated acid are that the anion is more water-soluble (less hydrophobic) and is repelled by the negatively charged surface.[18,19] The pH-sorption edge is modeled, showing a sharp drop in sorption inflecting at pH = pK_a. While the sorption of neutral NTO is, indeed, greater than the sorption of NTO^-, the difference is remarkably small—less than a factor of 4 in K_F and less than a factor of 2 in $S_{LM}{\cdot}K_L$ (Figure 3)—despite its charged and highly polar nature.

A potential contributing factor to the unexpectedly strong sorption of NTO^- by F400 is the formation of a (−)CAHB between NTO^- and appropriate acidic groups on the carbon surface, as noted in the Introduction. Behaviors characteristic of (−)CAHB complexation include[16,26] (1) enhanced sorption near the pH corresponding to the mean pK_a of solute and interacting surface groups(s), which is where complexation is expected to be maximal; (2) a shift in the apparent pK_a of the solute due to an increase in H-bond strength of the complex; (3) greater sorptive competition by a (−)CAHB-capable solute compared to a (−)CAHB-incapable solute; and (4) consumption of a proton from water if needed (eq 1). We evaluate the significance of these behaviors for NTO in the next three sections.

Sorption Edge. The pH profile of K_d, determined as single-point measurements, is shown in Figure 4. The plot has several important features. First, K_d values for neutral NTO at

https://doi.org/10.1021/acs.est.4c07055
Environ. Sci. Technol. 2024, 58, 20719−20728

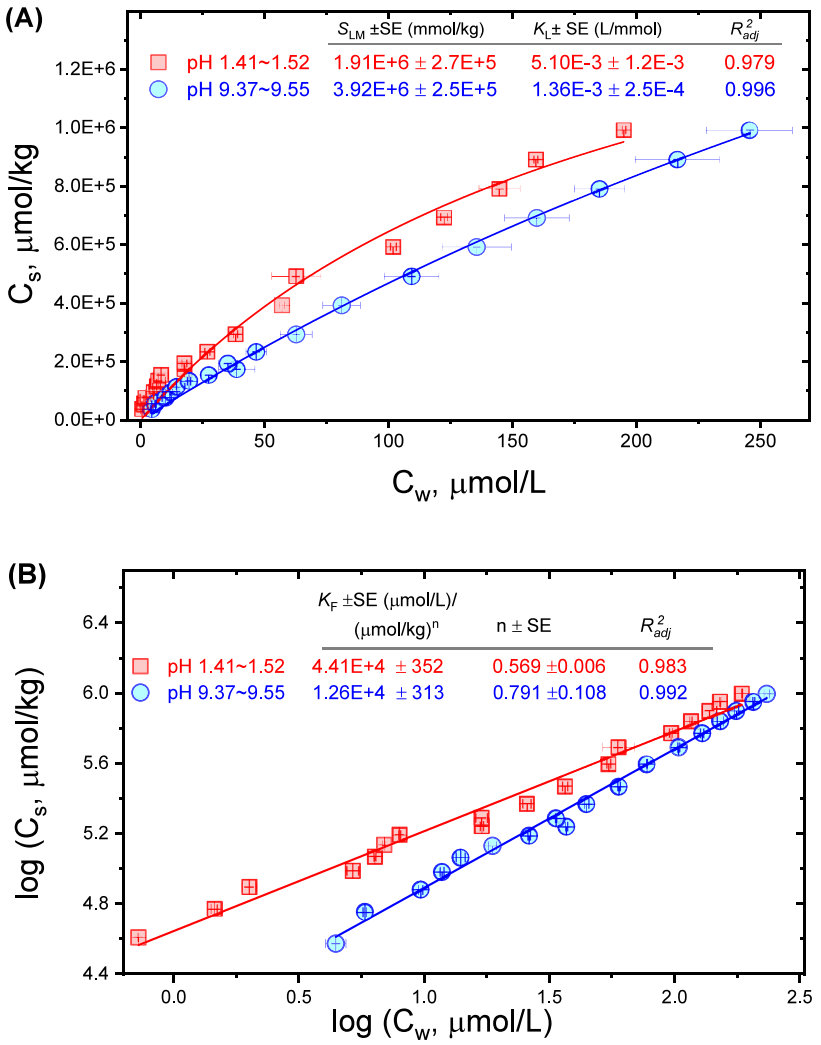

Figure 3. Sorption isotherms of NTO to F400 fit by the (A) Langmuir and (B) Freundlich models. Ionic strength, 125 mM (KCl); 25 C; 0.25 g/L F400. SD is standard error.

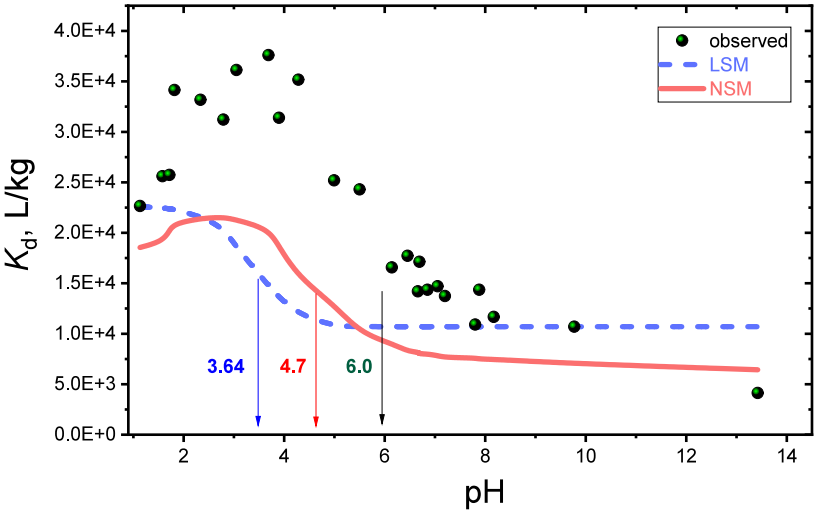

Figure 4. Adsorption edge of NTO on F400 (initial NTO = 50 μM) and curves for the linear (LSM) and nonlinear (NSM) speciation models. Arrows point to the approximate location of the inflection point for the experimental data as well as the locations of the calculated inflection points for the LSM and NSM models. The large "hump" in the data and the shift in the inflection point support the CAHB hypothesis.

low pH (≤2) are greater than those at higher pH (6−10), but by <2.5-fold. It should be noted that K_d at pH 5.5, where NTO^- represents 98.6% of total dissolved NTO, is nearly the same as that at pH 1, where neutral NTO represents 99.8% of

https://doi.org/10.1021/acs.est.4c07055
Environ. Sci. Technol. 2024, 58, 20719−20728

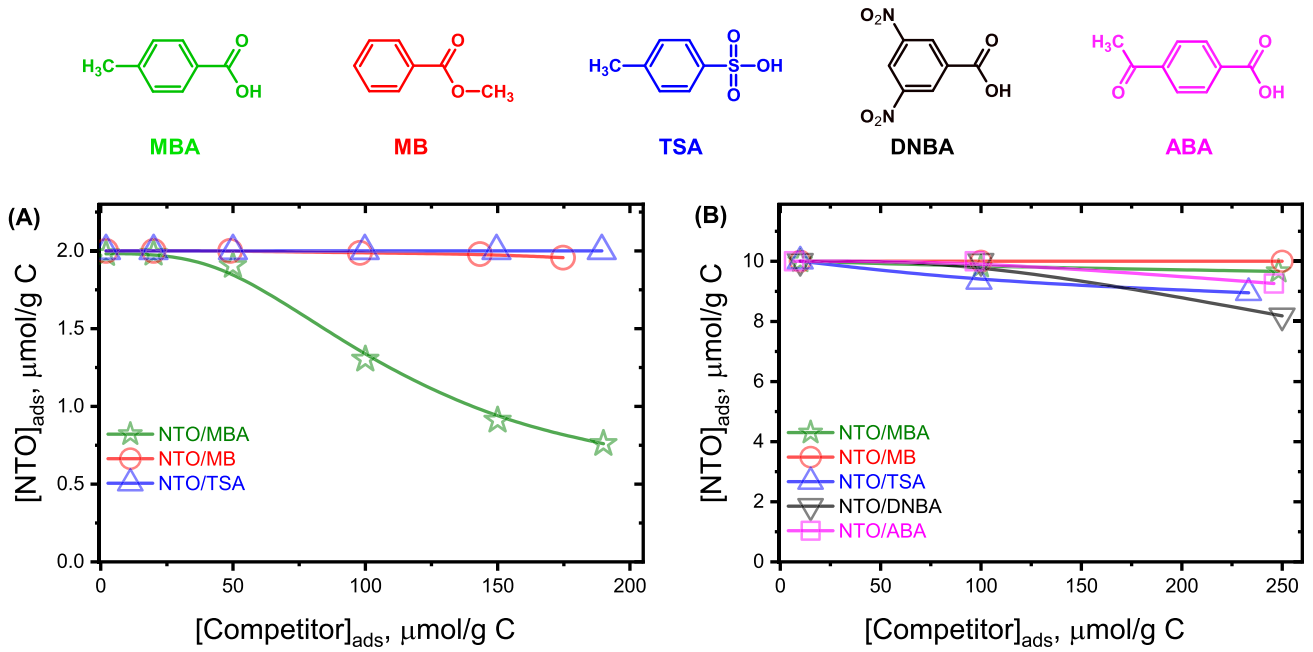

Figure 5. Bisolute competition experiments; sorbed concentration of NTO as a function of sorbed competitor concentration. (A) F400 = 5 g L^{-1} and (B) F400 = 1 g L^{-1}. Initial NTO concentration, 10 μM; initial competitor concentration, 10−950 μM; final pH, 6.41−6.82; ionic strength, 100 mM (NaCl).

total dissolved NTO. The small difference in K_d between neutral NTO and NTO^- is supportive of special interactions of NTO^-. The substantial drop in K_d above pH 10 can be explained by acid dissociation of NTO^- to give NTO^{2-} (eq 8; pK_{a2} = 11.08), which does not sorb significantly. In fact, making the solution alkaline (pH 13.8) can effectively reverse the sorption of NTO (Figure S5).

Second, the pH-K_d profile shows a large "hump" centered around pH 3−4. The formation of a CAHB between interacting species maximizes near the mean of their pK_a values. Thus, the hump appears at a pH near the mean pK_{a1} of NTO (3.64) and the putative pK_a of surface carboxyl groups (~3−6). Third, the pH-K_d scatterplot inflects at pH ~ 6—more than 2 units above the pK_{a1} of NTO. It is known that the pK_a of a CAHB complex exceeds the pK_a of either interacting group (by up to 3 units) because the proton is more tightly held in the complex.[26] Thus, both the large hump and shift in the inflection point are consistent with the (−)CAHB hypothesis.

Xiao and Pignatello found that a hump and an inflection point shift are also characteristic of extreme isotherm nonlinearity.[44] To see how this applies here, we compared the pH-K_d edge of NTO with two sorption-edge models—a linear and a nonlinear speciation model (LSM and NSM).[44] The governing relationship for the observed distribution coefficient is

$$K_{d,obs} = \frac{C_s^{ion} + C_s^{neut}}{C_w^{ion} + C_w^{neut}} \quad (9)$$

The LSM assumes that sorption is concentration-independent, i.e., $C_s^{ion} = K_d^{ion} C_w^{ion}$ and $C_s^{neut} = K_d^{neut} C_w^{neut}$, where K_d^{ion} and K_d^{neut} are the corresponding linear distribution coefficients, respectively. Thus,

$$K_{d,obs} = f^{ion} \cdot K_d^{ion} + f^{neut} \cdot K_d^{neut} \quad (10)$$

where f are mass fractions,

$$f^{ion} = \frac{1}{1 + 10^{-(pH - pK_{a1})}};\ f^{neut} = 1 - f^{ion} \quad (11)$$

The values of K_d^{ion} and K_d^{neut} were taken to be 1.07×10^4 and 2.27×10^4, respectively, i.e., those values represented by the experimental points at pH 9.77 and pH 1.13, respectively. Figure 4 plots the expected LSM relationship according to eqs 10 and 11 as the blue (dashed) curve. It predicts a smooth transition from K_d^{neut} to K_d^{ion}—i.e., no hump—and an inflection at pH = pK_{a1} of NTO. This is the classical interpretation of the sorption-pH edge trend for weak acids.[44]

The NSM[44] accounts for the concentration dependence of K_d. The Freundlich model can be used to account for nonlinearity. Substituting eq 1 (for C_s^{ion} or C_s^{neut}) and eq 11 into eq 10 gives,

$$K_{d,obs} = [(f^{ion})^{n^{ion}} \cdot K_F^{ion} \cdot (C_w^{n^{ion}-1})] + [(f^{neut})^{n^{neut}} \cdot K_F^{neut} \cdot (C_w^{n^{neut}-1})] \quad (12)$$

where K_F^{ion}, K_F^{neut}, n^{ion}, and n^{neut} are the Freundlich fitting parameters of neutral NTO at pH 1.5 for NTO^0 and pH 9.5 for NTO^- from Figure 3B. Figure 4 plots the expected relationship according to eq 12 as a red curve. The curve displays a small "hump" on the acidic pH side of the pK_{a1} and displacement of the inflection point from pH 3.64 to pH 4.7. The underlying cause of the hump and the inflection point shift relative to the ideal case (LSM), explained in detail previously,[44] is summarized as follows. As the pH approaches and crosses the pK_a from either direction, the aqueous concentration of the declining species (C_w^{neut} or C_w^{ion}) gradually decreases, while its corresponding K_d gradually increases due to the inherent nonlinearity of that species' isotherm.[44] We know that both NTO^- and neutral NTO give nonlinear isotherms on F400 (n = 0.791 and 0.569, respectively; Figure 3B). It should be noted that the experimental hump is much larger, and the inflection point shift is much greater than predicted by the NSM model. These results can be taken as

https://doi.org/10.1021/acs.est.4c07055
Environ. Sci. Technol. 2024, 58, 20719−20728

additional evidence for a third sorbed species, namely, a (−)CAHB complex of NTO^- with the surface acidic groups of F400.

Competitive Sorption. The degree of sorptive competitiveness depends on the relative single-solute sorption intensity of each compound and the degree of overlap in their sorption domains. Overlap can be limited by steric or electronic effects that limit or preclude the interaction of one compound relative to the other. Experiments were conducted wherein NTO was placed in competition with solutes capable of undergoing (−)CAHB, in comparison with solutes of similar steric sizes that are incapable of forming a (−)CAHB according to the ΔpK_a rule. MBA is capable of forming a (−)CAHB because its pK_a (4.26) is close to the pK_{a1} of NTO (3.64) and to intrinsic pK_a values of surface acidic groups that NTO is proposed to interact with via (−)CAHB. TSA has a pK_a (<0) quite far from those of normal acidic groups on the carbon and thus is not expected to interact appreciably with them by (−)CAHB. MB, the methyl ester of benzoic acid, exhibits no acid−base behavior in water and, therefore, is incapable of forming a (−)CAHB.

Figure 5A plots the sorbed concentration of NTO vs the sorbed concentration of MBA, MB, or TSA at pH 6.41−6.82. It reveals that only the (−)CAHB-capable competitor, MBA, displaces NTO, whereas the compounds incapable of forming (−)CAHB under those conditions, TSA and MB, do not. The lack of competition by TSA also argues against anion exchange, as strongly influential in NTO^- sorption. At higher sorbed NTO concentrations (Figure 5B), competition is expected to be weaker generally because less specific, lower-energy sites are involved in potential competition. Indeed, at 5-times higher NTO sorbed concentration, MBA is less effective, and MB is still completely ineffective at sorption suppression of NTO. TSA was slightly effective. Two other (−)CAHB-capable carboxylic acids, ABA (pK_a = 3.7) and DNBA (pK_a = 2.82), also show slight competitive pressure at the higher NTO concentration. Taken together, the results provide evidence consistent with the hypothesis that (−)CAHB contributes to NTO sorption.

To further investigate anion exchange, NTO^- was sorbed to quaternary ammonium (QA)-functionalized F400 in comparison with raw F400. The QA-functionalized sorbents include F400 coated with adsorbed polymer pDADMAC (F400-pDADMAC) or F400 chemically grafted with QA (F400-Q188 and F400-Q360). QA functionalization introduces positively charged sites (R_4N^+) on the carbon, imparting anion exchange capacity that is expected to enhance NTO^- sorption if anion exchange sorption was important. However, Figure 6 shows that NTO sorption at pH 7 is weaker for all of the QA-functionalized F400 carbon compared to raw F400. It is possible that the QA groups ion-pair with deprotonated acidic groups on the carbon, reducing or eliminating their ability to engage in (−)CAHB with NTO^-. Whatever the reason for the decline, the results argue against anion exchange playing a major role in NTO^- sorption to F400 and further support the hypothesis that (−)CAHB contributes to NTO sorption.

pH Drift. At intermediate pH values (e.g., 5.0), NTO and acidic groups on carbon are not fully dissociated. The proton of a new (−)CAHB between the two can be supplied by neutral NTO or the carbon itself, as has been demonstrated in other cases.[16,38] However, the (−)CAHB is sufficiently favorable that a proton can also be supplied by water, leading

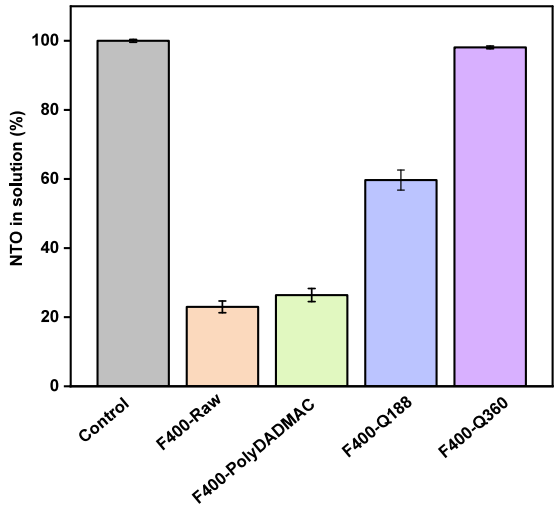

Figure 6. Sorption of NTO by F400 and quaternary ammonium-functionalized F400 sorbents. Concentration of NTO remaining in solution after 48 h of sorption was 12 g L^{-1} sorbent. Mixtures in water were stabilized at pH 7 (with small amount of HCl or NaOH) prior to NTO addition initially at 19.5 μM. No ionic strength adjustment.

to an increase in pH. Such a reaction for NTO may be written as follows,

$$NTO^- + H_2O + {}^-O\text{-}\blacksquare \rightarrow NTO^-\cdots H^+\cdots {}^-O\text{-}\blacksquare + OH^- \quad (13)$$

To test this hypothesis, we mixed a suspension of F400 in water with an NTO^- solution, each pre-equilibrated at pH 5, and then monitored the pH drift over 96 h. A control without NTO^- was also set up. The mixture of NTO^- and F400 should show pH drift, relative to the control, only if NTO^- and F400 interact in a way that consumes or generates H^+.

Figure 7 shows the pH of samples and controls with time at initial NTO concentrations of 500, 1000, and 2000 μM. The controls drift upward over the 96 h period, most likely due to the change in IS at t = 0. However, the pH values of the mixed samples drift upward further than the control at all three initial NTO concentrations. We take the difference in pH to signify the formation of a (−)CAHB with F400 accompanied by the release of hydroxide according to eq 13.

Some of the hydroxide released by reaction 12, however, is consumed by both F400 and neutral NTO due to their buffering capacities. The actual (corrected) hydroxide release ($M_{corr,t}$, mol/L) at each time t is given by,

$$M_{corr,t} = M_{obs,t} + M_{F400,t} + M_{NTO,t} \quad (14)$$

where $M_{obs,t}$ is the observed hydroxide released, $M_{F400,t}$ is the hydroxide consumed by F400, and $M_{NTO,t}$ is the hydroxide consumed by neutral NTO (see Text S1). $M_{obs,t}$ is calculated simply from the difference in the pH of the control (pH_t^{cont}) and sample (pH_t^{samp}). Values of $M_{NTO,t}$ are calculated from pK_{a1}, pH_t^{cont}, and pH_t^{samp} (eq S5). Values of $M_{F400,t}$ are computed from separately constructed base titration curves of F400 at each t (eq S9). An assumption is that NTO and F400 act as buffers independently.

A corrected pH (pH_t^{corr}) can be derived from $M_{corr,t}$ at each t. Figure 7 shows that pH_t^{corr} lies in the region of 8.39−9.41 and is much greater than the corresponding pH_t^{samp} at each initial NTO concentration and t. The fraction of NTO engaging in (−)CAHB with F400 and releasing hydroxide is given by,

https://doi.org/10.1021/acs.est.4c07055
Environ. Sci. Technol. 2024, 58, 20719−20728

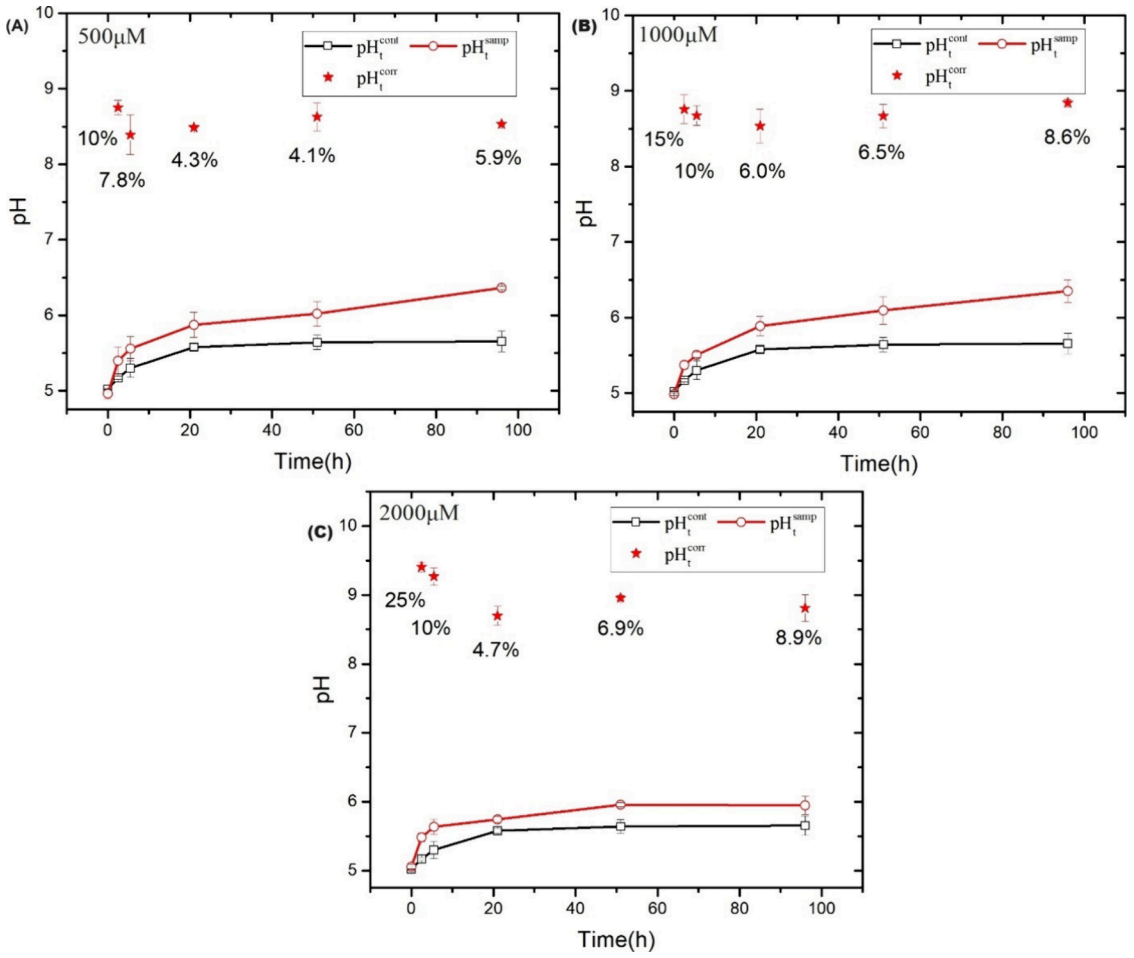

Figure 7. Results of the pH drift experiments. Solutions of NTO, NaCl, and F400 each pre-equilibrated to pH 5 and then combined at time zero. Final concentrations: 22.5 mg/L F400; 50 mM NaCl; and either 0 (^{cont}), 500, 1000, or 2000 μM NTO (^{samp}). The pH_t^{corr} refers to the value calculated after correction for buffering by F400 or NTO. The number beneath each datum is the fraction f_{CAHB} (%) of NTO engaged in CAHB with the release of a hydroxide (range of duplicates <1% of average).

$$f_{CAHB} = \frac{M_{corr,t}}{NTO_{sorb,t} \cdot S_{F400}} \quad (15)$$

where $NTO_{sorb,t}$ (mol/g) is the sorbed concentration at t, and S_{F400} (g/L) is the F400 concentration. The values listed in Figure 7 adjacent to the respective pH_t^{corr} point indicate that the fraction of NTO that associates with F400 in this way ranges from 4.1 to 25% and increases slightly with nominal NTO concentration. The results of the pH drift experiment are consistent with the CAHB hypothesis.

This study has rigorously examined the sorption behavior of NTO on carbon, showing that the strong sorption of NTO, despite its anionic and highly polar nature, can be explained in part by the formation of an exceptionally strong H-bond of the charge-assisted type with surface acidic groups. Other forces, such as dispersion, induction, and electrostatic, obviously also contribute. Anion exchange does not appear to play a major role in this case. The study also precisely determined the pK_a values of this diprotic acid using both spectrophotometric and potentiometric methods.

The findings are novel and significant. It is the first time that the CAHB has been identified as a participant in the adsorption of an ionizable compound to a high-temperature ("activated") carbon. In addition, this is the first time that the CAHB has been identified in the interaction of an ionizable urea moiety with a carbonaceous material. We have applied a novel approach for identifying the CAHB consisting of evaluating isotherms, pH-adsorption edge plots, competitive sorption experiments, and pH drift experiments. The findings are significant because they contradict conventional thoughts that polar organic anions have little affinity for—indeed, are repelled by—hydrophobic carbonaceous sorbents. Models for the sorption of ionizable compounds must be modified to take into consideration their potential for CAHB formation with the sorbent. The findings advance our understanding of the sorption of ionizable compounds to carbon and have especially important implications for the use of carbon in environmental remediation and catalysis. For NTO specifically, the results are relevant to the design of strategies for mitigating its mobility in soil at production, military training, and battlefield sites and recovering it from contaminated water. They are also relevant to the design and use of carbonaceous catalysts for the removal of NTO, a topic we will report on in the near future.

■ ASSOCIATED CONTENT

Supporting Information

The Supporting Information is available free of charge at https://pubs.acs.org/doi/10.1021/acs.est.4c07055.

Spectrophotometric and potentiometric titration plots, sorption and extraction profiles for NTO recovery

https://doi.org/10.1021/acs.est.4c07055
Environ. Sci. Technol. 2024, 58, 20719−20728

experiments, and calculations related to corrected pH for pH drift experiments (PDF)

AUTHOR INFORMATION

Corresponding Author

Joseph J. Pignatello − *Department of Environmental Science and Forestry, The Connecticut Agricultural Experimental Station, New Haven, Connecticut 06511, United States;* orcid.org/0000-0002-2772-5250; Email: Joseph.Pignatello@ct.gov

Authors

Wael Abdelraheem − *Department of Environmental Science and Forestry, The Connecticut Agricultural Experimental Station, New Haven, Connecticut 06511, United States;* Present Address: Centers for Disease Control and Prevention (CDC), National Institute for Occupational Safety and Health (NIOSH), Health Effects Laboratory Division (HELD), and Chemical and Biological Monitoring Branch (CBMB), 1090 Tusculum Avenue, Cincinnati, Ohio 45226, United States; orcid.org/0000-0003-4390-7756

Lingjun Meng − *Department of Environmental Science and Forestry, The Connecticut Agricultural Experimental Station, New Haven, Connecticut 06511, United States;* Present Address: School of Civil and Environmental Engineering, Georgia Institute of Technology, Atlanta, Georgia 30332, United States.

Nourin Seenthia − *Department of Civil and Environmental Engineering, Villanova University, Villanova, Pennsylvania 19085, United States*

Wenqing Xu − *Department of Civil and Environmental Engineering, Villanova University, Villanova, Pennsylvania 19085, United States;* orcid.org/0000-0002-9838-8220

Complete contact information is available at: https://pubs.acs.org/10.1021/acs.est.4c07055

Author Contributions

[§]W.A. and L.M. contributed equally to this work.

Notes

The authors declare no competing financial interest.

ACKNOWLEDGMENTS

Support was provided by the U.S. Department of Defense (DoD) through the Strategic Environmental Research and Development Program (SERDP) under ER19-1239.

REFERENCES

(1) Ahmad, M.; Rajapaksha, A. U.; Lim, J. E.; Zhang, M.; Bolan, N.; Mohan, D.; Vithanage, M.; Lee, S. S.; Ok, Y. S. Biochar as a sorbent for contaminant management in soil and water: a review. *Chemosphere* **2014**, *99*, 19−33.

(2) Mohan, D.; Sarswat, A.; Ok, Y. S.; Pittman, C. U. Organic and inorganic contaminants removal from water with biochar, a renewable, low cost and sustainable adsorbent - A critical review. *Bioresour. Technol.* **2014**, *160*, 191−202.

(3) Hadi, P.; Yeung, K. Y.; Barford, J.; An, K. J.; McKay, G. Significance of "effective" surface area of activated carbons on elucidating the adsorption mechanism of large dye molecules. *Journal of Environmental Chemical Engineering* **2015**, *3* (2), 1029−1037.

(4) Pauletto, P. S.; Lütke, S. F.; Dotto, G. L.; Salau, N. P. G. Adsorption mechanisms of single and simultaneous removal of pharmaceutical compounds onto activated carbon: Isotherm and thermodynamic modeling. *J. Mol. Liq.* **2021**, *336*, No. 116203.

(5) Ahnert, F.; Arafat, H. A.; Pinto, N. G. A study of the influence of hydrophobicity of activated carbon on the adsorption equilibrium of aromatics in non-aqueous media. *Adsorption* **2003**, *9*, 311−319.

(6) Dąbrowski, A.; Podkościelny, P.; Hubicki, Z.; Barczak, M. Adsorption of phenolic compounds by activated carbon—a critical review. *Chemosphere* **2005**, *58* (8), 1049−1070.

(7) Lin, D.; Xing, B. Adsorption of phenolic compounds by carbon nanotubes: role of aromaticity and substitution of hydroxyl groups. *Environ. Sci. Technol.* **2008**, *42* (19), 7254−7259.

(8) Schwarzenbach, R. P.; Gschwend, P. M.; Imboden, D. M. *Environmental Organic Chemistry*; Wiley: 2016.

(9) Sigmund, G.; Arp, H. P. H.; Aumeier, B. M.; Bucheli, T. D.; Chefetz, B.; Chen, W.; Droge, S. T. J.; Endo, S.; Escher, B. I.; Hale, S. E.; Hofmann, T.; Pignatello, J.; Reemtsma, T.; Schmidt, T. C.; Schönsee, C. D.; Scheringer, M. Sorption and Mobility of Charged Organic Compounds: How to Confront and Overcome Limitations in Their Assessment. *Environ. Sci. Technol.* **2022**, *56* (8), 4702−4710.

(10) Anniyappan, M.; Talawar, M. B.; Sinha, R. K.; Murthy, K. P. S. Review on Advanced Energetic Materials for Insensitive Munition Formulations. *Combustion, Explosion, and Shock Waves* **2020**, *56* (5), 495−519.

(11) Sokkalingam, N.; Potoff, J. J.; Boddu, V. M.; Maloney, S. W.; Baird, J. C. *Prediction of Environmental Impact of High-Energy Materials with Atomistic Computer Simulations*; U.S. Army Engineer Research and Development Center: Champaign, IL, 2010.

(12) Spear, R. J.; Louey, C. N.; Wolfson, M. G. *A Preliminary Assessment of 3-Nitro-1,2,4-triazol-5-one (NTO) as an Insensitive High Explosive*; DSTO Materials Research Laboratory Maribyrnong: Australia, 1989.

(13) Ariyarathna, T.; Twarz, S.; Tobias, C. Adsorption and Removal Kinetics of 2, 4-Dinitroanisole and Nitrotriazolone in Contrasting Freshwater Sediments: Batch Study. *Environ. Toxicol. Chem.* **2023**, *42* (1), 46−59.

(14) Mark, N.; Arthur, J.; Dontsova, K.; Brusseau, M.; Taylor, S. Adsorption and attenuation behavior of 3-nitro-1, 2, 4-triazol-5-one (NTO) in eleven soils. *Chemosphere* **2016**, *144*, 1249−1255.

(15) Linker, B. R.; Khatiwada, R.; Perdrial, N.; Abrell, L.; Sierra-Alvarez, R.; Field, J. A.; Chorover, J. Adsorption of novel insensitive munitions compounds at clay mineral and metal oxide surfaces. *Environmental Chemistry* **2015**, *12* (1), 74−84.

(16) Li, X.; Pignatello, J. J.; Wang, Y.; Xing, B. New insight into adsorption mechanism of ionizable compounds on carbon nanotubes. *J. Environ. Sci. Technol.* **2013**, *47* (15), 8334−8341.

(17) Moreno-Castilla, C. Adsorption of organic molecules from aqueous solutions on carbon materials. *Carbon* **2004**, *42* (1), 83−94.

(18) Ayranci, E.; Duman, O. Adsorption of aromatic organic acids onto high area activated carbon cloth in relation to wastewater purification. *Journal of Hazardous Materials* **2006**, *136* (3), 542−552.

(19) Ward, T. M.; Getzen, F. M. Influence of pH on the adsorption of aromatic acids on activated carbon. *Environ. Sci. Technol.* **1970**, *4* (1), 64−67.

(20) Gilli, G.; Gilli, P. Towards an unified hydrogen-bond theory. *J. Mol. Struct.* **2000**, *552* (1), 1−15.

(21) Gilli, G.; Gilli, P. *The Nature of the Hydrogen Bond: Outline of a Comprehensive Hydrogen Bond Theory*; Oxford University Press: 2009; Vol. 23.

(22) Gilli, P.; Pretto, L.; Bertolasi, V.; Gilli, G. Predicting hydrogen-bond strengths from acid−base molecular properties. The pKa slide rule: Toward the solution of a long-lasting problem. *Acc. Chem. Res.* **2009**, *42* (1), 33−44.

(23) Perrin, C. L. Are Short, Low-Barrier Hydrogen Bonds Unusually Strong? *Acc. Chem. Res.* **2010**, *43* (12), 1550−1557.

(24) Mariam, Y. H.; Musin, R. N. Transition from Moderate to Strong Hydrogen Bonds: Its Identification and Physical Bases in the Case of O−H···O Intramolecular Hydrogen Bonds. *J. Phys. Chem. A* **2008**, *112* (1), 134−145.

(25) Pakiari, A. H.; Eskandari, K. The chemical nature of very strong hydrogen bonds in some categories of compounds. *Journal of Molecular Structure: THEOCHEM* **2006**, *759* (1), 51−60.
(26) Ni, J.; Pignatello, J. Charge-assisted hydrogen bonding as a cohesive force in soil organic matter: water solubility enhancement by addition of simple carboxylic acids. *Jornal of Environmental Science: Processes Impacts* **2018**, *20* (9), 1225−1233.
(27) Li, X.; Gámiz, B.; Wang, Y.; Pignatello, J. J.; Xing, B. Competitive Sorption Used To Probe Strong Hydrogen Bonding Sites for Weak Organic Acids on Carbon Nanotubes. *Environ. Sci. Technol.* **2015**, *49* (3), 1409−1417.
(28) Ni, J.; Pignatello, J. J.; Xing, B. Adsorption of aromatic carboxylate ions to black carbon (biochar) is accompanied by proton exchange with water. *Environ. Sci. Technol.* **2011**, *45* (21), 9240−9248.
(29) Teixidó, M.; Pignatello, J. J.; Beltrán, J. L.; Granados, M.; Peccia, J. Speciation of the Ionizable Antibiotic Sulfamethazine on Black Carbon (Biochar). *Environ. Sci. Technol.* **2011**, *45* (23), 10020−10027.
(30) Xiao, F.; Pignatello, J. J. Effects of Post-Pyrolysis Air Oxidation of Biomass Chars on Adsorption of Neutral and Ionizable Compounds. *Environ. Sci. Technol.* **2016**, *50* (12), 6276−6283.
(31) Hsieh, H.-S.; Pignatello, J. Activated carbon-mediated base hydrolysis of alkyl bromides. *Applied Catalysis B: Environmental* **2017**, *211*, 68−78.
(32) Kraft, A. The Determination of the pKa of Multiprotic, Weak Acids by Analyzing Potentiometric Acid-Base Titration Data with Difference Plots. *J. Chem. Educ.* **2003**, *80* (5), 554.
(33) Birdi, K. *Surface and Colloid Chemistry*. CRC Press: 2003; pp 664−669.
(34) Lee, K.-Y.; Chapman, L. B.; Cobura, M. D. 3-Nitro-1, 2, 4-triazol-5-one, a less sensitive explosive. *Journal of Energetic Materials* **1987**, *5* (1), 27−33.
(35) Le Campion, L.; Adeline, M.; Ouazzani, J. Separation of NTO Related 1, 2, 4-Triazole-3-One Derivatives by a high performance liquid chromatography and capillary electrophoresis. *Propellants, Explosives, Pyrotechnics* **1997**, *22* (4), 233−237.
(36) Smith, M. W.; Cliff, M. D. *NTO-Based Explosive Formulations: A Technology Review*; DSTO Aeronautical and Maritime Research Laboratory: Australia, 1999.
(37) Golius, A.; Gorb, L.; Michalkova Scott, A.; Hill, F. C.; Leszczynski, J. Computational study of NTO (5-nitro-2,4-dihydro-3H-1,2,4-triazol-3-one) tautomeric properties in aqueous solution. *Structural Chemistry* **2015**, *26* (5), 1281−1286.
(38) Murillo-Gelvez, J.; Di Toro, D. M.; Allen, H. E.; Carbonaro, R. F.; Chiu, P. C. Reductive Transformation of 3-Nitro-1,2,4-triazol-5-one (NTO) by Leonardite Humic Acid and Anthraquinone-2,6-disulfonate (AQDS). *Environ. Sci. Technol.* **2021**, *55* (19), 12973−12983.
(39) Kofman, T. P.; Pevzner, M. S.; Zhukova, L. N.; Kravchenko, T. A.; Frolova, G. M. Methylation of 3-Nitro-1,2,4-Triazol-5-One. *Russ. J. Org. Chem.* **1980**, *16*, 420.
(40) Harris, N. J.; Lammertsma, K. Tautomerism, Ionization, and Bond Dissociations of 5-Nitro-2,4-dihydro-3H-1,2,4-triazolone. *J. Am. Chem. Soc.* **1996**, *118* (34), 8048−8055.
(41) Schroer, H. W.; Londono, E.; Li, X.; Lehmler, H.-J.; Arnold, W.; Just, C. L. Photolysis of 3-Nitro-1, 2, 4-triazol-5-one: Mechanisms and Products. *ACS EST Water* **2023**, *3* (3), 783−792.
(42) Kosmulski, M. The pH dependent surface charging and points of zero charge. X. Update. *Adv. Colloid Interface Sci.* **2023**, *319*, No. 102973.
(43) Mahmudov, R.; Huang, C. P. Perchlorate removal by activated carbon adsorption. *Sep. Purif. Technol.* **2010**, *70* (3), 329−337.
(44) Xiao, F.; Pignatello, J. J. Effect of Adsorption Nonlinearity on the pH−Adsorption Profile of Ionizable Organic Compounds. *Langmuir* **2014**, *30* (8), 1994−2001.

https://doi.org/10.1021/acs.est.4c07055
Environ. Sci. Technol. 2024, 58, 20719−20728